UKACC International Conference on Control 2012
Cardiff, UK, 3-5 September 2012

An Algorithm for Generating Real Describing Functions

G.F.Page, J.B.Gomm and S.S.Douglas
School of Engineering, Technology & Maritime Operations
Liverpool John Moores University
Liverpool, UK
g.f.page@ljmu.ac.uk

Abstract— A classical method of dealing with the non-linear elements in a transfer function is to assume that they can be separated from the linear section and can then be represented by describing functions. The standard method of calculating these describing functions has been to use a graphical method which breaks the non-linear characteristic into a series of linear sections and super-imposes their effects onto a sinusoidal input. The output is assumed to be a Fourier series and the Fourier transform for the first coefficient of this series is calculated in a piecemeal fashion. The process is not difficult but there is a considerable amount of calculation involved. In this paper an algorithm is presented which enables the describing functions of real non-linearities, with any number of linearized sections, to be simply written down without the usual onerous calculations. Additionally, a method of quickly sketching the general shape of describing functions is outlined.

Keywords- non-linearity; describing function; limit-cycle.

I. INTRODUCTION

This paper begins by outlining the standard graphical method for obtaining describing functions and then proceeds to use the technique to develop a general solution for obtaining the family of real describing functions. These are the describing functions whose non-linear characteristics are the same irrespective of whether the magnitude of the input signal is increasing or decreasing. Obtaining a general solution also permits the creation of algorithms for its implementation and one such algorithm is presented. Although the general methods of deriving complex describing functions are well known, the real describing functions have usually been overlooked in the literature or else have been considered as trivial. This has meant that some simplifying approaches, and their associated algorithms, have been overlooked.

The purpose of developing a general method is to enable the easy and rapid delineation of the describing functions for real non-linearities – these are non-linearities which do not possess memory. To demonstrate the effectiveness of the general method, and the associated algorithm that has also been developed, the describing functions for two common linearities have been calculated: one which caused a single limit-cycle to be produced and one which caused two limit-cycles. The predicted limit-cycle results obtained by applying the algorithm were compared with simulations using SIMULINK.

II. THE GRAPHICAL METHOD

The early development of the graphical describing function technique can be traced to several groups working independently [1], [2], [3], [4]. However these wartime developments did not come into general use until the mid - 1950s [4], [5], [8]. It is basically an harmonic balance approach modified for feedback control. This meant that only the principal harmonic was used and higher-order oscillations were considered to be negligible due to the filtering influence of the inertia inherent in the overall process which was being controlled. The basic graphical approach is shown in Figure 1. It is assumed that the input is sinusoidal (bottom left-hand corner of the diagram) and this is mapped via the non-linearity (represented at the top left-hand corner of the diagram) to an output. The input has an input magnitude *x* plotted against time *t*. The non-linear transformation translates this input magnitude *x*, on the horizontal axis, to the output magnitude *y* on the vertical axis. The output is a plot of output *y* against time *t*. This is the same time period as for the input signal and hence the output signal *y*, due to the non-linear transformation is correlated with the input.

Assuming a sinusoidal input, the input equation will be given by:

$$x = X.\sin(\omega t) \tag{1}$$

Since the non-linearity is symmetric about the origin, and since most systems behave like low-pass filters because of inertia, the output equation will be given by:

$$y = A_1 \sin(\omega t) \tag{2}$$

Hence the describing function is

$$N(X,\omega) = \frac{A_1}{X} \tag{3}$$

and there is only a need to calculate A_1.

Also, because of the quarter–wave symmetry:

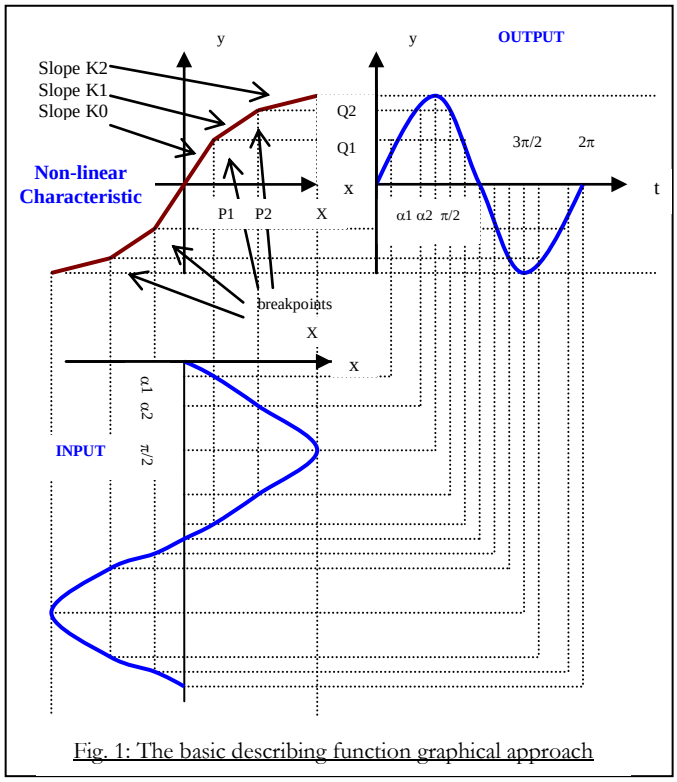

Fig. 1: The basic describing function graphical approach

$$A_1 = \frac{4}{\pi}\int_0^{\frac{\pi}{2}} y.\sin(\omega t).d(\omega t) \qquad (4)$$

The method is a quasi-linearization process in which a section of a static non-linearity is represented by a gain which depends on the magnitude of the input signal [6], [7], [9]. For this reason it is assumed that the non-linearity consists of lines of constant slope to each side of the break-points. The integrations can be calculated in a piecewise fashion to give:

$$A_1 = \frac{4}{\pi}\left[\int_0^{\alpha_1} y.\sin(\omega t).d(\omega t) + \int_{\alpha_1}^{\alpha_2} y.\sin(\omega t).d(\omega t) + \int_{\alpha_2}^{\frac{\pi}{2}} y.\sin(\omega t).d(\omega t)\right] \qquad (5)$$

where the individual values of y in each of the separate linear sections have the form

$$y = Kx + c \qquad (6)$$

in which K is the slope of the relevant section. The positions at which the slopes K abruptly change value have been termed ***break-points*** in this investigation.

A. A General Solution

Gibson and subsequent authors [7], [8], [9] showed how to obtain a general approach to the calculation of describing function by using this piecewise linear approach but aimed for an overall solution involving both real and imaginary parts. Also, although the early authors developed a general approach they only applied it case-by-case and did not present a general algorithm It is our opinion that a useful general algorithm can be obtained by considering single-valued non-linearities separately from double, or multi-valued, non-linearities and then specifically formulating a general solution. Single-valued non-linearities will produce real, as opposed to complex, describing functions and they can often be described by polynomial functions. By using this approach a general method for generating the describing functions of real non-linearities has been obtained. This work has resulted in a straightforward and relatively simple method of generating describing functions. An added advantage is that since there will be no phase-shifts, the superposition of the inverse Nyquist locus onto the describing function diagram is simplified since only one value of the inverse Nyquist locus, that at which it crosses the real axis, will need to be considered.

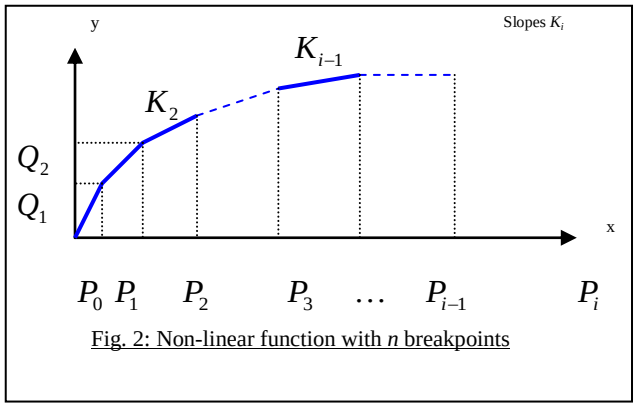

Fig. 2: Non-linear function with *n* breakpoints

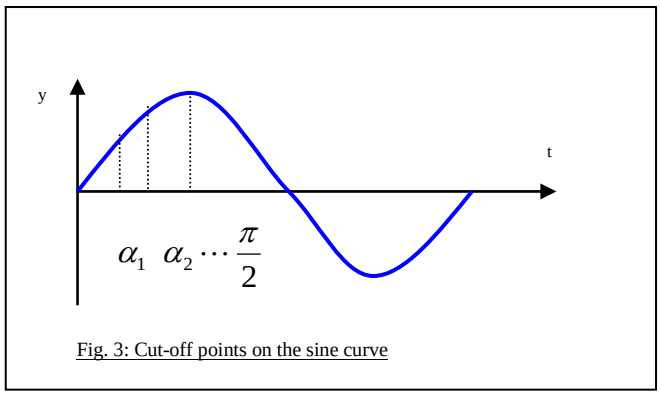

Fig. 3: Cut-off points on the sine curve

By taking Gibson's initial construction, in Fig. 1, with two breakpoints and extending it to *n* breakpoints the graph will have (*n* - 1) linear sections with slopes $K_0 K_1 \ldots K_n$, and breakpoints occurring at horizontal positions $P_1 P_2 \ldots P_n$ (with P_0 at the origin if necessary), jumps in the vertical plane (y-direction) at $Q_1 Q_2 \ldots$ and angles on the sinusoidal input of $\alpha_1 \alpha_2 \ldots \alpha_i \ldots \alpha_n, \frac{\pi}{2}$. The non-linearity will have the form shown in Fig. 2 (replacing the on-linear characteristic, top left-

GP would like to thank Prof. Ian Jenkinson, School of Engineering, Liverpool John Moores University for the facilities and support which enabled this work to be undertaken.

hand corner of Fig. 1 which maps the input signal to the output signal)**.** The cut-off points on the sine curve will occur

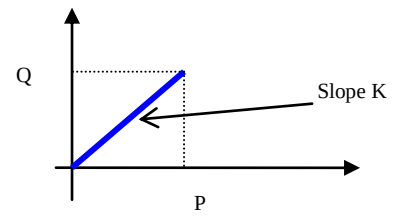

Fig. 4: Relationship between P and Q

as in Fig. 3 (replacing the sinusoidal-type of output in the top right-hand corner of Fig. 1.) The calculation of A_1 will be given:

$$A_1 = \frac{4}{\pi}\left[\begin{array}{l}\int_0^{\alpha_1} y.\sin(\omega t).d(\omega t) + \int_{\alpha_1}^{\alpha_2} y.\sin(\omega t).d(\omega t) + \ldots \\ \ldots + \int_{\alpha_{i-1}}^{\alpha_i} y.\sin(\omega t).d(\omega t) + \ldots + \int_{\alpha_n}^{\pi/2} y.\sin(\omega t).d(\omega t)\end{array}\right] \quad (6)$$

which produces a general solution for the describing function:

$$N = \frac{2}{\pi}\left[K_n.\frac{\pi}{2} + \sum_{i=1}^{n}(K_{i-1} - K_i)\left(\sin^{-1}\left(\frac{P_i}{X}\right) + \left(\frac{P_i}{X}\right)\sqrt{\left[1-\left(\frac{P_i}{X}\right)^2\right]}\right)\right] \quad \textbf{(7)}$$

If Coulomb friction or relay action is present at initial amplitudes then equation (7) has to be adjusted.

Consider the case where only Coulomb friction is present: as $P \to 0 \;\; y = Q$, Fig. 4, $K_0 = \infty \;\; and \;\; K_1 = 0$.

In this case, as $P \to 0, \sin^{-1}\left(\frac{P}{X}\right) \to \frac{P}{X}$ and

$$\left(\frac{P}{X}\right)\sqrt{\left[1-\left(\frac{P}{X}\right)^2\right]} \to \frac{P}{X}$$

Also from Figure (4), $P = \frac{Q}{K}$

Hence equation (7) reduces to $N = \frac{4Q}{\pi X}$ (8).

B. An Algorithm

An algorithm for using the general solution given in equation (7) and the special case of equation (8) to generate particular real describing functions is now presented. Although it specifically deals with discrete cases it can easily be extended to deal with continuous functions.

If Coulomb friction or relay action is present, start at stage one, otherwise start at stage two.

Stage One:

(a) If Coulomb friction or relay action is present then make $\frac{4Q}{\pi X}$ the first term of the describing function, where Q is the value of the Coulomb friction term.

(b) If dead-zone is also present multiply the above result by $\sqrt{\left[1-\left(\frac{P}{X}\right)^2\right]}$ where P is the dead-zone break-point.

Stage Two:

(a) If saturation is not present make K_n the first term of the describing function. (K_n is the gain of the last stage of the non-linearity) or add it to the result of stage one.

(b) If saturation is present then omit this term.

Stage Three:

(a) If there are n breakpoints then add n terms of the form

$$\frac{2}{\pi}(K_{i-1} - K_i)\left(\sin^{-1}\left(\frac{P_i}{X}\right) + \left(\frac{P_i}{X}\right)\sqrt{\left[1-\left(\frac{P_i}{X}\right)^2\right]}\right)$$

$$where\; i = 0 \to n.$$

Go to end.

(b) If saturation is present then change the last of the terms in stage 3(a) to

$$\frac{2}{\pi}K_{n-1}\left(\sin^{-1}\left(\frac{P_{n-1}}{X}\right) + \left(\frac{P_{n-1}}{X}\right)\sqrt{\left[1-\left(\frac{P_{n-1}}{X}\right)^2\right]}\right)$$

Go to end.

End.

III. Derivation of Two Describing Functions Using the Algorithm

Two examples are presented (i) dead-zone plus saturation which can cause a single limit-cycle to be produced and (ii) a non-linearity which has three break-points (four pseudo-linear regions) and so can cause two nested limit-cycles to be produced. The effects of these non-linearities were then simulated by placing them in series with a transfer function for a third-order linear system and applying unity feedback. The simulations were created using the SIMULINK package.

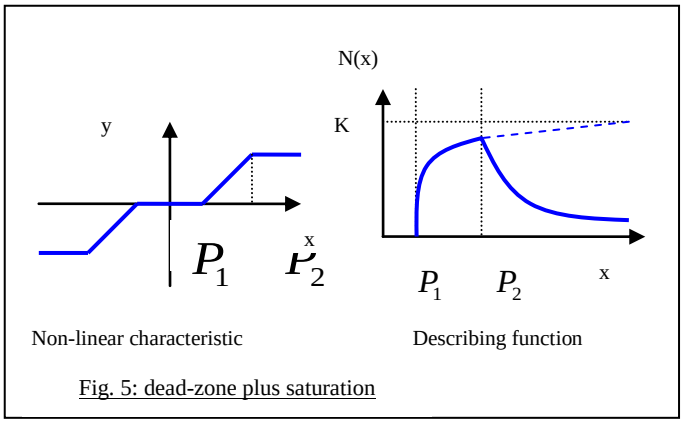

Fig. 5: dead-zone plus saturation

A. *Dead-zone plus saturation*

The parameters are $n = 2, K_0 = 0, K_1 = K, K_2 = 0$ so equation (7) gives:

$$N = \frac{2K}{\pi}\left[\sin^{-1}\left(\frac{P_2}{X}\right) - \sin^{-1}\left(\frac{P_1}{X}\right) + \left(\frac{P_2}{X}\right)\sqrt{\left[1-\left(\frac{P_2}{X}\right)^2\right]} - \left(\frac{P_1}{X}\right)\sqrt{\left[1-\left(\frac{P_1}{X}\right)^2\right]}\right]$$

when $X > P_2$; N as for deadzone when $P_1 < X \le P_2$ and $N = 0$ when $X \le P_1$

Using the algorithm, stages two (b), three (a) and three (b) apply and give the same result as above. This result is shown graphically in Fig. 5.

B. *A non-linearity with three break-points (four slopes)*

In this case only one combination of slopes of the pseudo-linear sections has been considered: $K_0 > K_1 \,\&\, K_1 < K_2 \,\&\, K_2 > K_3$.

In particular, $K_0 = -0.7, K_1 = 0.2, K_2 = 1.5 \,\&\, K_3 = 0.2$.

Again, the results were obtained by using equation (7), and by the algorithm, to give

$$N = \frac{2}{\pi}\left[\begin{array}{l} K_3.\frac{\pi}{2} + (K_2 - K_3)\left[\sin^{-1}\left(\frac{P_3}{X}\right) + \left(\frac{P_3}{X}\right)\sqrt{\left[1-\left(\frac{P_3}{X}\right)^2\right]}\right] + \ldots \\ (K_1 - K_2)\left[\sin^{-1}\left(\frac{P_2}{X}\right) + \left(\frac{P_2}{X}\right)\sqrt{\left[1-\left(\frac{P_2}{X}\right)^2\right]}\right] + \ldots \\ (K_0 - K_1)\left[\sin^{-1}\left(\frac{P_1}{X}\right) + \left(\frac{P_1}{X}\right)\sqrt{\left[1-\left(\frac{P_1}{X}\right)^2\right]}\right] \end{array}\right]$$

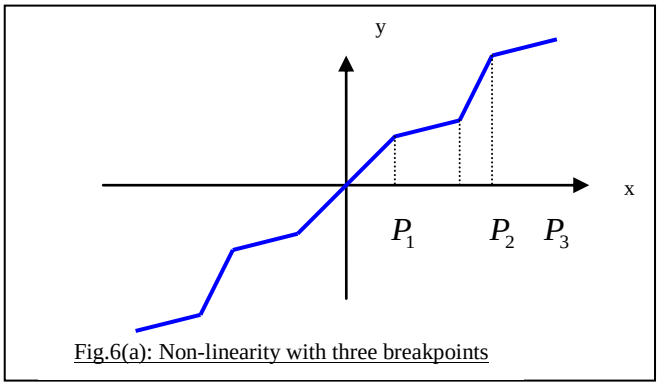

Fig.6(a): Non-linearity with three breakpoints

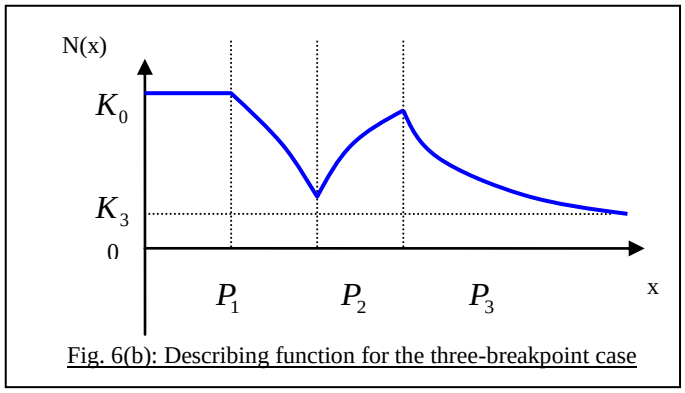

Fig. 6(b): Describing function for the three-breakpoint case

Using the algorithm, stages two (a) and three (a) apply. The graphical results are shown in Fig. 6(a) and Fig. 6(b).

IV. Use of Real Describing Functions to Predict Limit-Cycles

If the describing function is represented by N(X,ω) and the open-loop transfer function of a system is represented by G(jω) the Kochenburger's Stability Criterion [4] states that, in order for a system to remain stable, the locus $|G(j\omega)|$ must keep the entire locus $-1/|N(X,\omega)|$ on the right; or the inverse locus $1/|G(j\omega)|$ must keep the locus $-|N(X,\omega)|$ on the left (or must completely enclose the whole of the locus). For this work the authors found that the inverse Nyquist approach was more convenient. Furthermore, since only systems with real, as opposed to complex, describing functions were being investigated, plots with real and imaginary axes were of little use. It was better to plot the magnitude of the describing functions against the magnitude of the input signal and to superimpose on this the magnitude of the inverse Nyquist value at which it crossed the real axis. The position at which the descending describing function locus crossed the inverse Nyquist value then enabled the magnitude of the limit-cycle to be determined – as shown in Fig. 7.

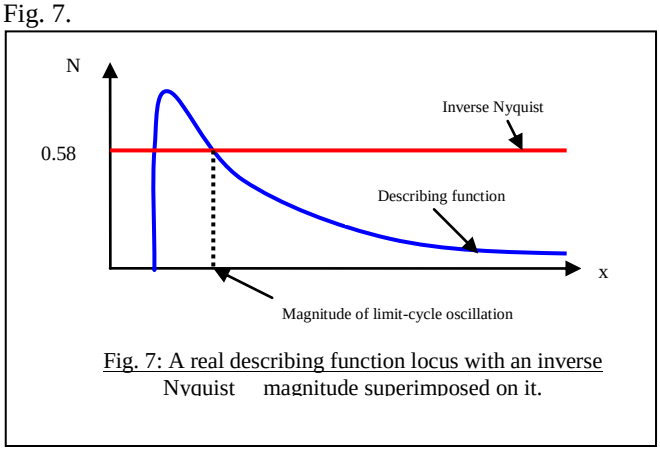

Fig. 7: A real describing function locus with an inverse Nyquist magnitude superimposed on it.

A similar approach was tried [10] using the direct Nyquist instead of the inverse function but it didn't lend itself to the same predictive opportunities.

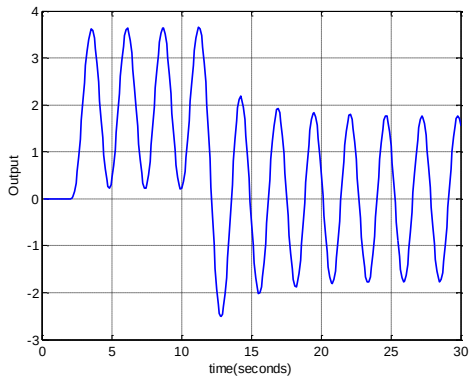

Fig. 8: Limit-cycle oscillation with saturation and dead-zone

A. *Dead-zone plus saturation*

According to the basic describing function locus shown in Fig. 5 this has the potential to exhibit the limit-cycle effect. The system was simulated in series with a third-order transfer function and the oscillatory response shown in Fig. 8 was obtained. This oscillatory response was produced with the limits of the saturation non-linearity set to ±1 and dead-zone set to ±0.5.

The calculated magnitude of the limit-cycle, from Fig. 10, is 1.79 ± 0.02. The actual magnitude of the limit-cycle, from Fig. 9, is 1.78 ± 0.03. The calculated frequency of oscillation is 2.45±0.001 rad/s and, from Figure 9 the measured frequency of oscillation is 2.44 ± 0.03 rad/s

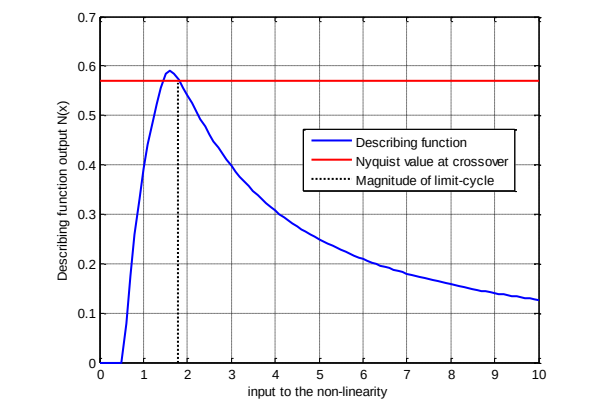

Fig. 9: Plot of describing function of dead-zone plus saturation

B. *The non-linearity with three break-points (four slopes)*

This time there were two positions where limit-cycles might occur depending on the signal input magnitude.

From Fig. 10, the measured frequency of the limit-cycle oscillation was 2.41 ± 0.07 rad/s which compared with the calculated limit-cycle frequency of 2.45 ± 0.001 rad/s. From Figure 11 the calculated magnitude of the lower limit-cycle was 1.60 ± 0.05 and of the higher limit-cycle it was 9.2 ± 0.08. From Fig. 10 the actual magnitude of the lower limit-cycle was 1.52 ± 0.7 and of the higher limit-cycle it was 10.1 ± 1.2.

It was found, by successively increasing the values of the second impulse magnitude, that the second limit-cycle was reached once the impulse had been raised above about 5.6, although it took several oscillation to reach this new stable position. Again, this could be predicted from Figure 11 where the rising value of the describing function crossed the Inverse Nyquist.

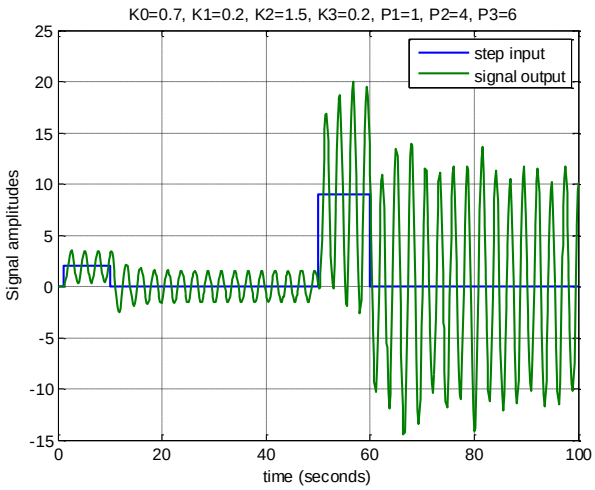

Fig. 10: The three-breakpoint response showing two limit-cycles

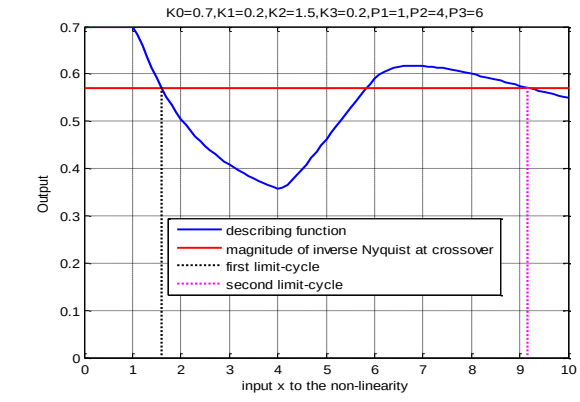

Fig.11: Describing function for the three break-point characteristic

V. A QUICK METHOD OF SKETCHING DESCRIBING FUNCTIONS

In every case investigated, both in those shown in Figures 5 and 6(b) and in more complicated real non-linearities, the slope of the 'linear' section became the asymptotic value to which that section of the describing function tended. Also, there was an abrupt change in the describing function at the same value of x as that at which the break-value of the non-linearity occurred. When $|K_n| > |K_{n-1}|$ the locus increased in value approximately to the formula: $y = K_{n-1} + (K_n - K_{n-1})(1 - e^{-x})$ and when $|K_n| < |K_{n-1}|$ the locus decreased in value approximately to the formula: $y = K_n + (K_{n-1} - K_n)e^{-x}$. A more precise mathematical description of each type of locus was not considered necessary since the observed behaviour has only been used in subsequent work to afford a rough sketch of the shape of the describing function. A sketch can be performed more rapidly than using the algorithm to give a general outline of the shape before the algorithm itself is used to give more precise results.

VI. CONCLUDING REMARKS

This work has used the classical method for deriving describing functions. However, by restricting the formulation to deal only with those non-linearities which produce real, not complex, describing functions it has been possible to devise an algorithm which enabled such functions to be simply written down without the usual onerous calculations. Furthermore, the method could be rapidly applied to non-linearities of considerable complexity. Also, because only real describing functions were being considered, it was possible to use a simplified graphical form of Kochenburger's criteria to derive the positions of limit-cycles and also the range of inputs needed to induce them. After the derivation of the algorithm two examples of non-linearities have been presented, one which produces a single limit-cycle and one which produces two nested limit-cycles. The expected parameters which produced these effects have been calculated and compared with the actual results obtained by simulation. Finally a quick method of producing a rough sketch of the general shape of a describing function has been included. This paper presents the first stages of a series of investigations into non-linear effects and their control.

REFERENCES

[1] Tustin, A., The effects of backlash and of speed dependent friction on the stability of closed cycle control systems, JIEE, part II, Vol. 94, pp 143-151, 1947.

[2] Dutilh, J., Theorie des servomechanism a relais, Onde Elec., pp 438-445, 1950.

[3] Oppelt, W., Locus curve method for regulators with friction, Z. Deut. Ingr., Berlin, p 90, 1948.

[4] Kochenburger, R.J., A frequency response method for analysing and synthesising contactor servomechanisms, Trans. AIEE, Vol. 69, pp 270-283, 1950.

[5] Atherton, D.P., Nonlinear Control Engineering, Van Nostrand, 1975.

[6] Atherton, D.P., Stability of Non-Linear Systems, Research Studies Press, Wiley, 1981.

[7] Gibson, J.E., Nonlinear Automatic Control, McGraw-Hill, New York, pp 405-410, 1963.

[8] Khalil, H.K., Non-linear System 3rd Ed., Prentice-Hall, pp 54-59, 280-288, 2002.

[9] Dutton, K., Thompson, S. and Barraclough, , B., The Art of Control Enginerering, Prentice-Hall, pp 698-710 , 1997.

[10] Kim, E., Lee, H., and Park, M., Limit-Cycle Prediction of a Fuzzy Control System Based on Describing Function Method, IEEE Trans. Fuzzy Systems, Vol. , No. 1, pp 11-22, 2000.